Electronic Supplementary Material (ESI) for Journal of Materials Chemistry A.
This journal is © The Royal Society of Chemistry 2019

Supporting Information

Gas Transport Regulatory in MO/MOF Interface for Enhanced Selective Gas Detection

Ming-Shui Yao,[+a] Lin-An Cao,[+a, c] Yong-Xiang Tang,[b] Guan-E Wang,[a] Rui-Heng Liu,[a] P Naresh Kumar,[a] Guo-Dong Wu,[a] Wei-Hua Deng,[a] Wen-Jing Hong,*[b] and Gang Xu*[a, c]

[a] State Key Laboratory of Structural Chemistry, Fujian Institute of Research on the Structure of Matter, Chinese Academy of Sciences (CAS), 155 Yangqiao Road west, Fuzhou, Fujian, 350002, P.R.China

[b] College of Chemistry and Chemical Engineering, Xiamen University, 422 Siming South Road, Xiamen 361005, China (P. R. China)

[c] University of Chinese Academy of Sciences (UCAS), No.19A Yuquan Road, Beijing 100049, China (P. R. China)

E-mail: whong@xmu.edu.cn (W.-J. Hong), gxu@fjirsm.ac.cn (G. Xu)

Linear discriminant analysis (LDA)

Linear discriminant analysis (LDA) was empolied to statistically analyze the sensing data, the result of which can provide a quantitative indication of the ability of the sensors in distinguishing among different VOCs. With LDA, the sensing data were associated with predetermined groups, and new cases can be classified into those groups. Three discriminant functions (response, response time and recovery time) were employed to classify the target gases into two groups (acetone and interfering gases).

1. **Calculate the average m_i**

$$m_i = (\mu_1, \mu_2, ..., \mu_j)$$

Where i is the classes of gases, m_1=acetone, m_2=interfering gases; j is the number of variables (1=response, 2=response time, 3=recovery time).

2. Calculate the intra-/inter-class scatter matrix

within-class scatter matrix

$$S_W = \sum_{i=1}^{c} S_i$$

Where

$$S_i = \sum_{k=1}^{N_i} (x_k - m_i)(x_k - m_i)^T$$

$$m_i = \frac{1}{N_i} \sum_{k=1}^{N_i} x_k$$

between-class scatter matrix

$$S_B = \frac{\sum_{i=1}^{c} [N_i (m_i - m)(m_i - m)^T]}{\sum_{i=1}^{c} N_i}$$

Where, c is the number of categories, the value of c is 2, m is a vector which has three values and show the average of all samples in each variables, m_i is similar with m and shows the average of each variables in category i, N_i is the number of sample in category i, x_k is the vector of sample k in category i which has three variables.

3. Calculate eigenvalues and eigenvectors

$$S_W^{-1} S_B$$

Since eigenvalues are sorted in descending order, the greatest amount of data variance will be closed. The corresponding eigenvector is W.

4. Calculate the new matrix

$$Y_i = X_i \times W$$

Where i is the classes of gases

5. The test sample can be assigned into one of the two available classes in new space depends on its Euclidean distances with training samples.

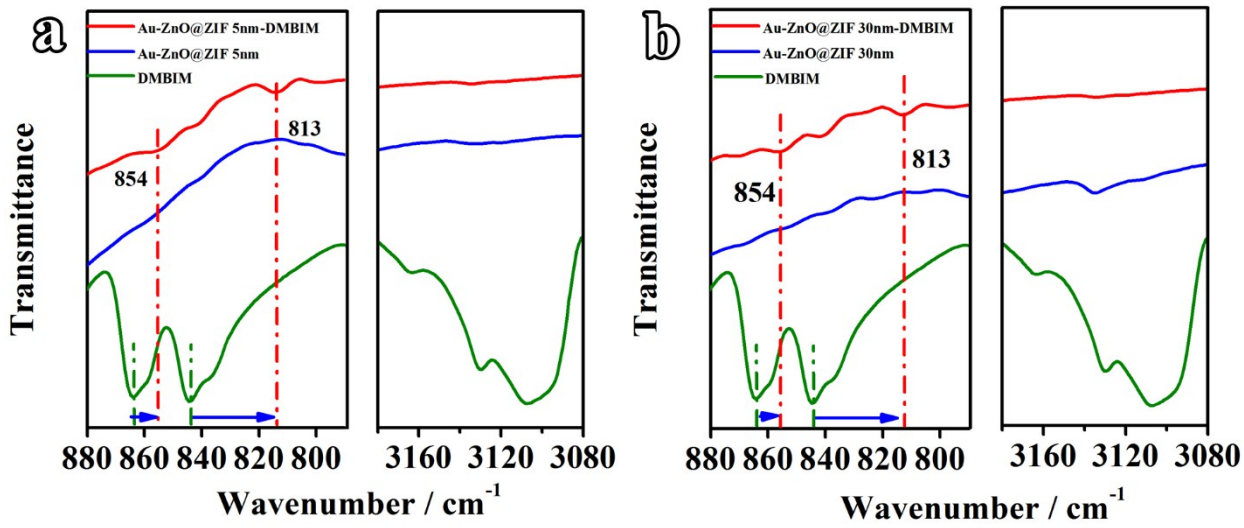

Fig.S1 FTIR spectra of DMBIM ligand, (a)Au-ZnO@ZIF 5 nm and (b)Au-ZnO@ZIF 50 nm-DMBIM

New peaks (813 cm^{-1} and 854 cm^{-1}) correspond to the C-H out-of-plane deformation vibrations in the phenyl rings of DMBIM. The red shift of these two peaks and the disappearance of N-H stretching vibrations at 3100 cm^{-1} are attributed to the deprotonation of DMBIM and subsequent Zn-DMBIM coordination.

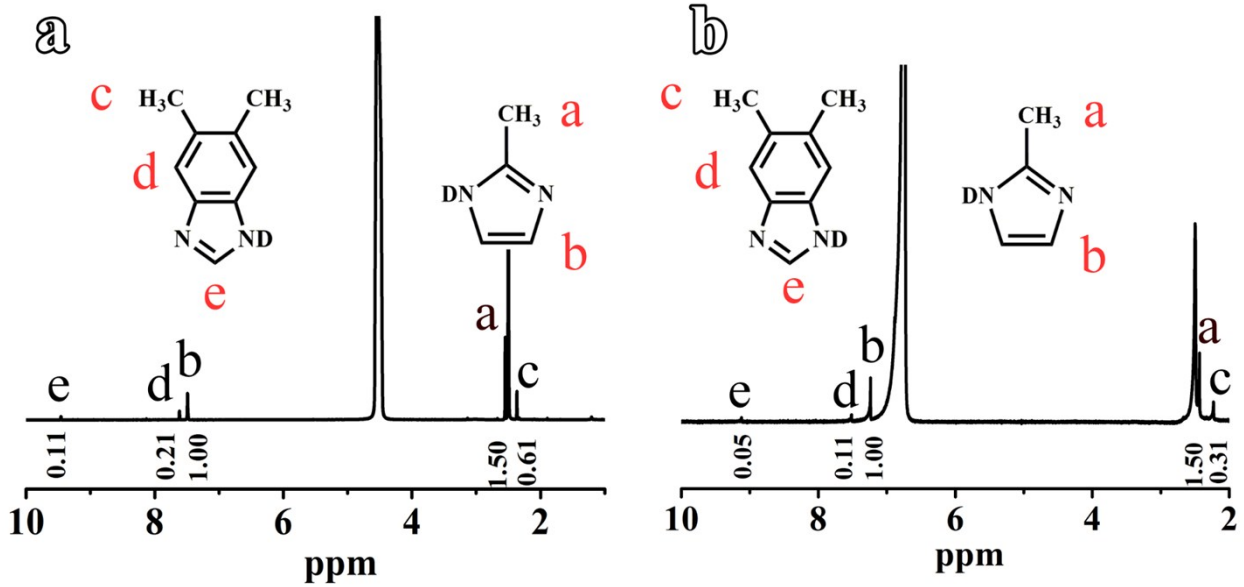

Fig.S2 ^{1}H-NMR spectra of the dissolved (a) ZnO@ZIF 5 nm-DMBIM and (b) ZnO@ZIF 50 nm-DMBIM

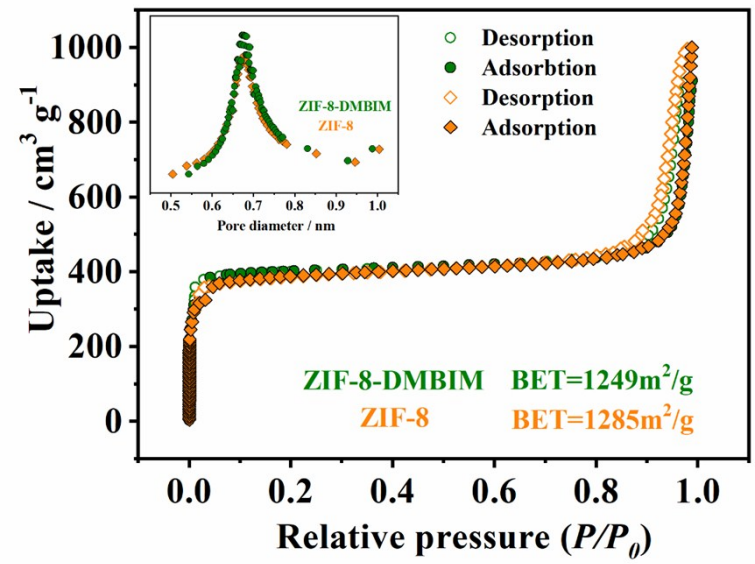

Fig.S3 N_2 sorption isotherms of ZIF-8 and ZIF-8-DMBIM (the inset: pore size analysis)

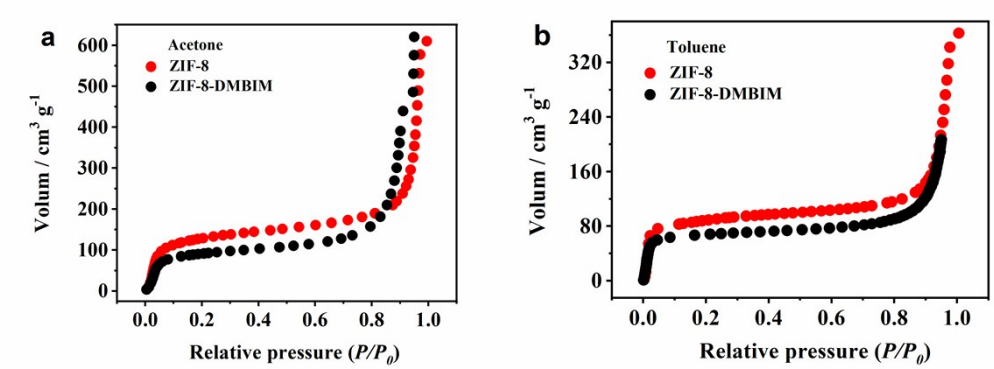

Fig.S4 (a) Acetone and (b) Toluene vapor sorption measurements of ZIF-8 and ZIF-8-DMBIM at room temperature

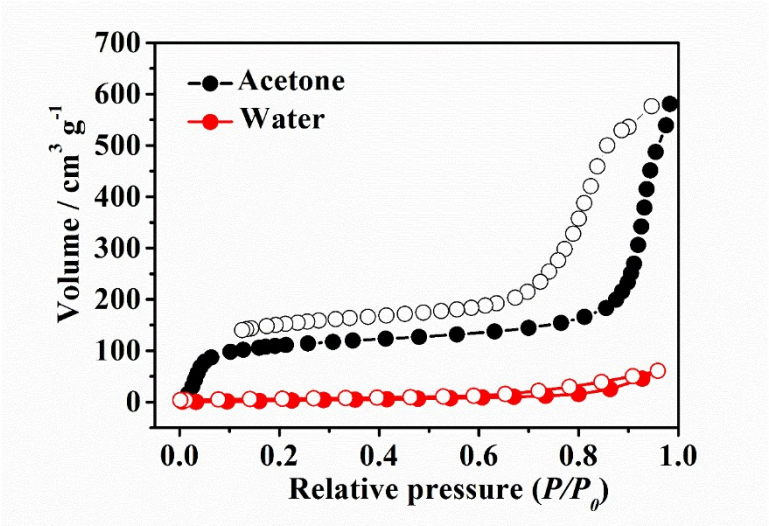

Fig.S5 Acetone and water vapor sorption measurements of ZIF-8-DMBIM at room temperature

Table S1. Physical parameters of selected gas and vapor adsorbates.

Sample	D_k [a] / nm	Molecular cross-sectional area / nm^2	Vapor sorption volume [b] / $cm^3\ g^{-1}$	Vapor sorption reduction [c] / %
acetone	0.47	0.26	186.7 / 157.1	16
toluene	0.585	0.344	112.6 / 86.7	23
ethylbenzene	0.60	0.378	95.9 / 53.6	44

[a] Gas molecules are expected to be spheres. [b] ZIF-8 / ZIF-8-DMBIM (P/P_0=0.8). [c] Vapor sorption of ZIF-8-DMBIM compared with ZIF-8.

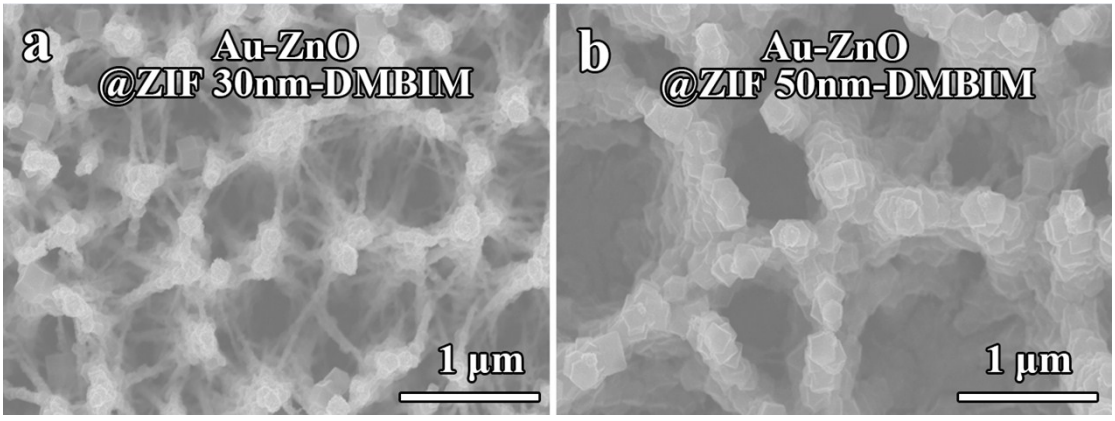

Fig.S6 SEM images of (a) Au-ZnO@ZIF 30 nm-DMBIM and (b) Au-ZnO@ZIF 50 nm-DMBIM

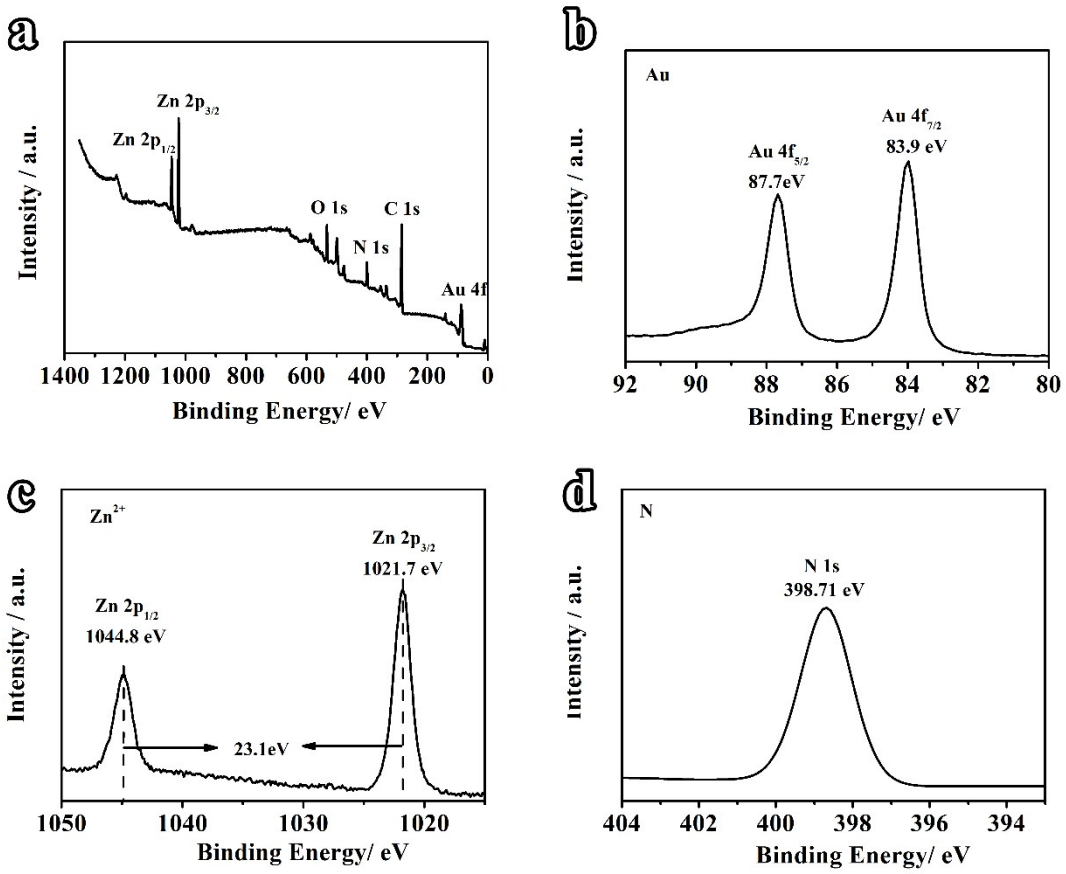

Fig.S7 (a) XPS patterns of Au-ZnO@ZIF 30 nm-DMBIM; (b)-(d) high resolution XPS patterns of Au-ZnO@ZIF 30 nm-DMBIM corresponding to Au 4f, Zn 2p, and N1s respectively

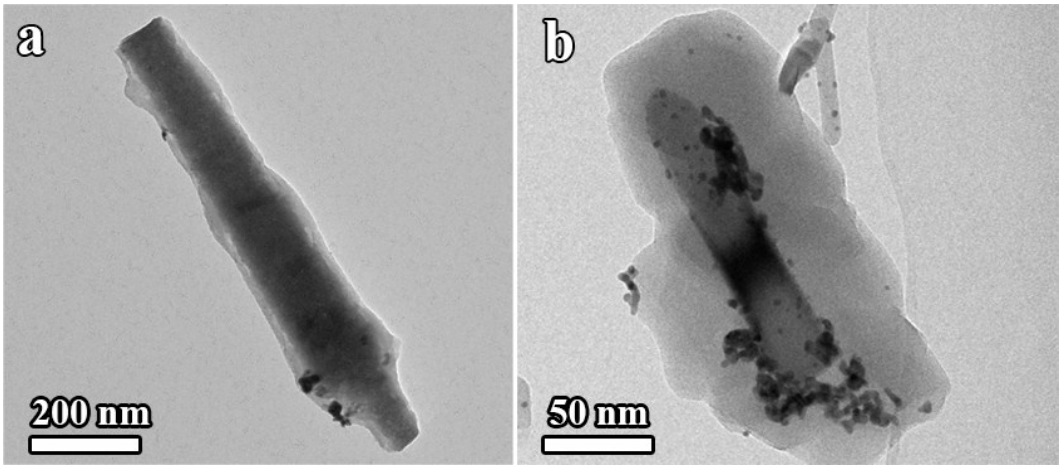

Fig.S8 TEM images of (a) Au-ZnO@ZIF 30 nm and (b) Au-ZnO@ZIF 50 nm

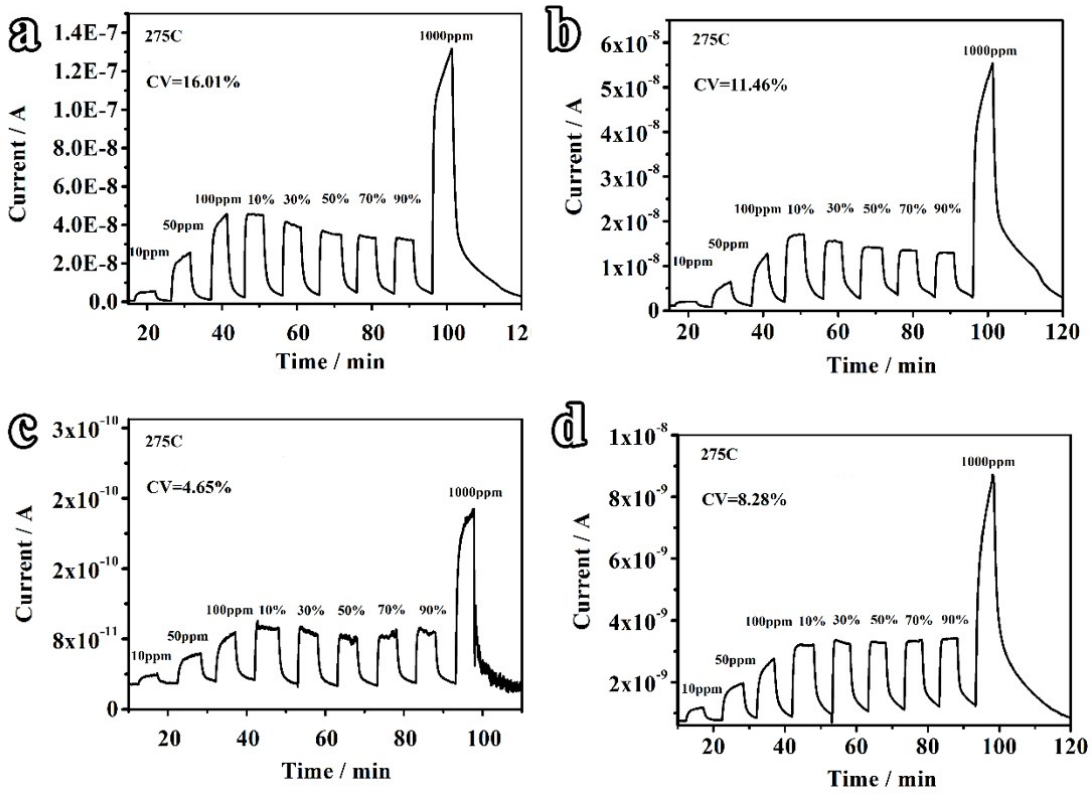

Fig.S9 Response-recovery curves of (a) Au-ZnO@ZIF 5 nm (b) Au-ZnO@ZIF 5 nm DMBIM (c) Au-ZnO@ZIF 50 nm (d) Au-ZnO @ZIF 50 nm-DMBIM at 275°C to 100 ppm acetone with different relative humidity

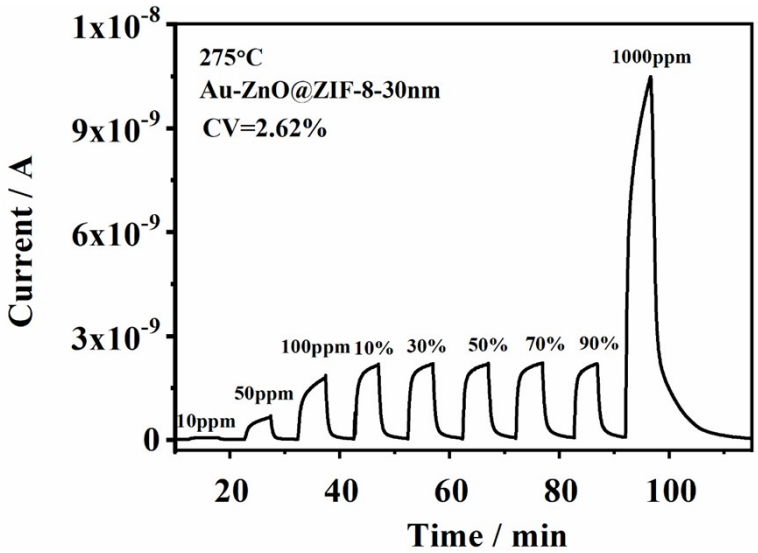

Fig.S10 Response-recovery curves of Au-ZnO@ZIF 30 nm at 275°C to 100 ppm acetone with different relative humidity

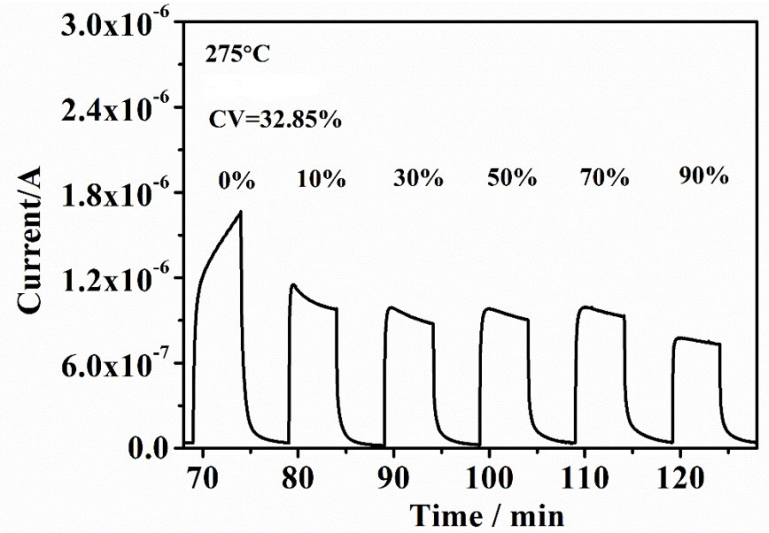

Fig.S11 The response-recovery curve of Au-ZnO to 100 ppm acetone with different relative humidity.

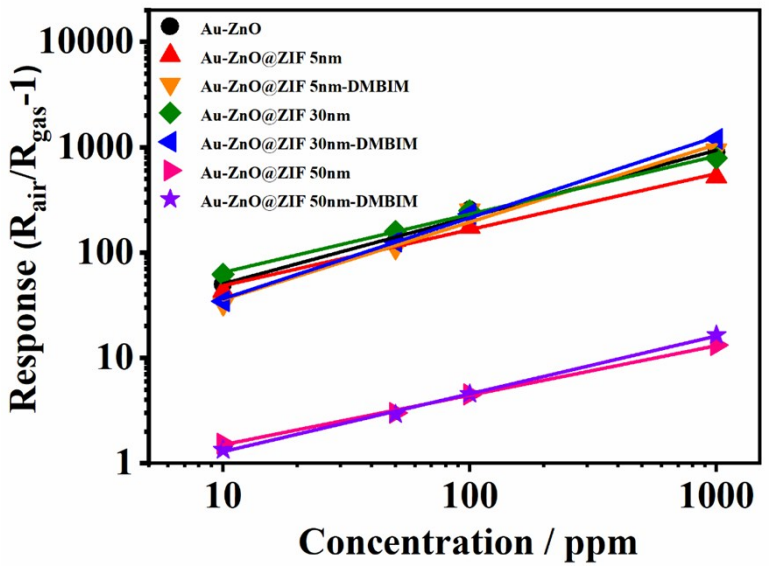

Fig.S12 Response-concentration log-log plots comparison of different sensors.

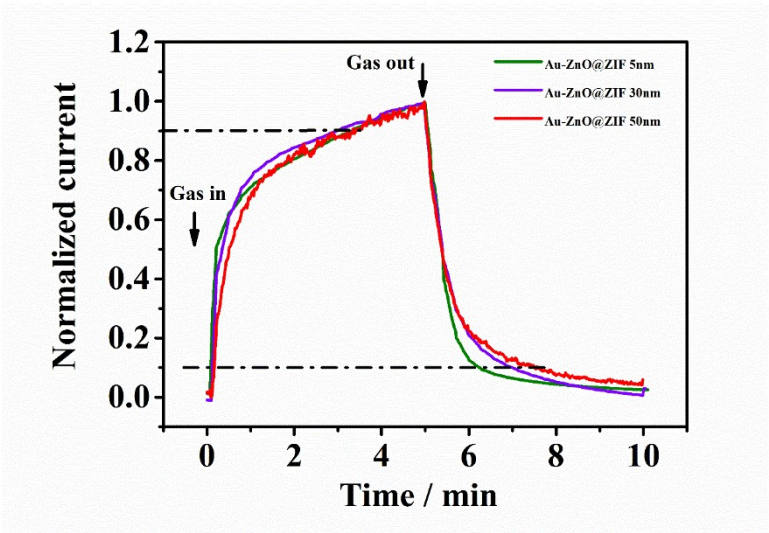

Fig.S13 Normalized response-recovery curves of Au-ZnO@ZIF to 100 ppm acetone at 275°C

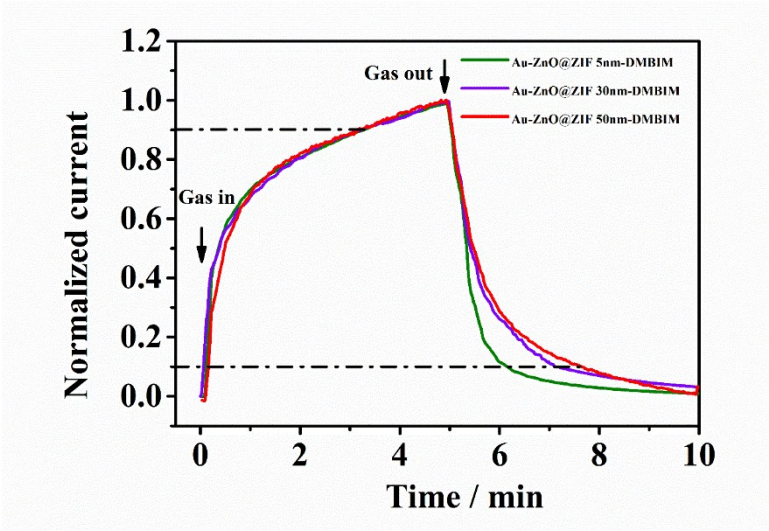

Fig.S14 Normalized response-recovery curves of Au-ZnO@ZIF-DMBIM to 100 ppm acetone at 275°C.

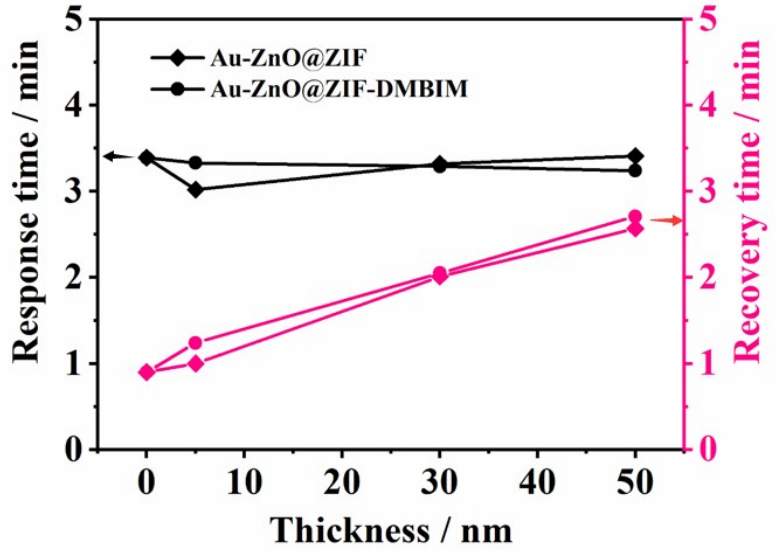

Fig.S15 Response and recovery time comparison of different sensors

These materials also have similar response & recovery speeds with the reasonable values of ~3 and ~1 min, respectively, in the situation of the chamber residence time of ~0.5 min.

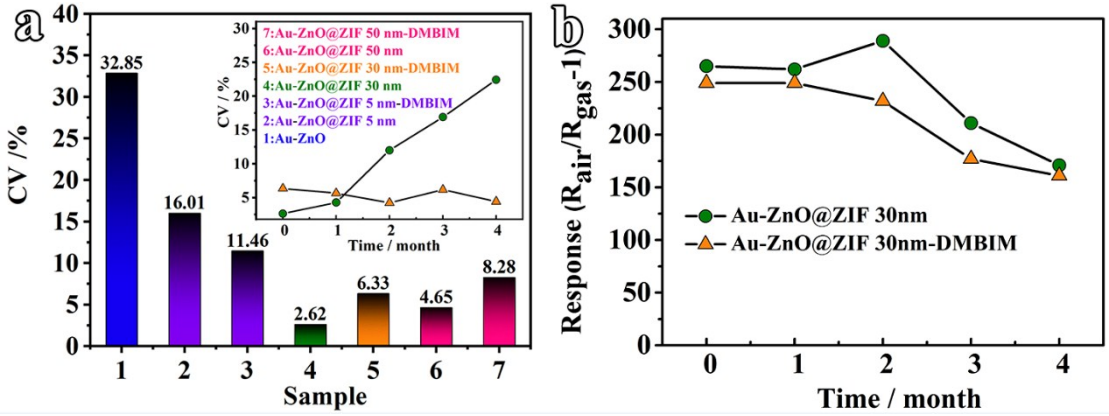

Fig.S16 (a) CV comparison of the sensors by varying RH from 0 to 90% (acetone 100 ppm, inset: long-term stability of anti-humidity properties), and (b) response long-term stability of Au-ZnO@ZIF 30 nm and Au-ZnO@ZIF 30 nm-DMBIM for 4 months.

As for response long-term stability, both Au-ZnO@ZIF 30 nm and Au-ZnO@ZIF 30 nm-DMBIM can keep 65% of original response value after 4 month exposing to the air (Figure S16b).

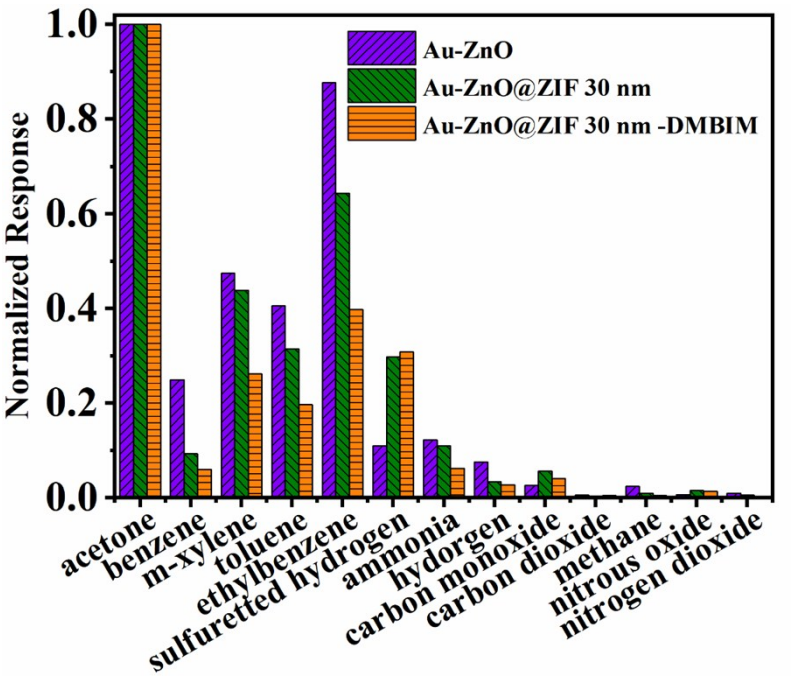

Fig.S17 Normalized response comparison of Au-ZnO, Au-ZnO@ZIF 30 nm and Au-ZnO@ZIF 30 nm-DMBIM toward various interfering gases

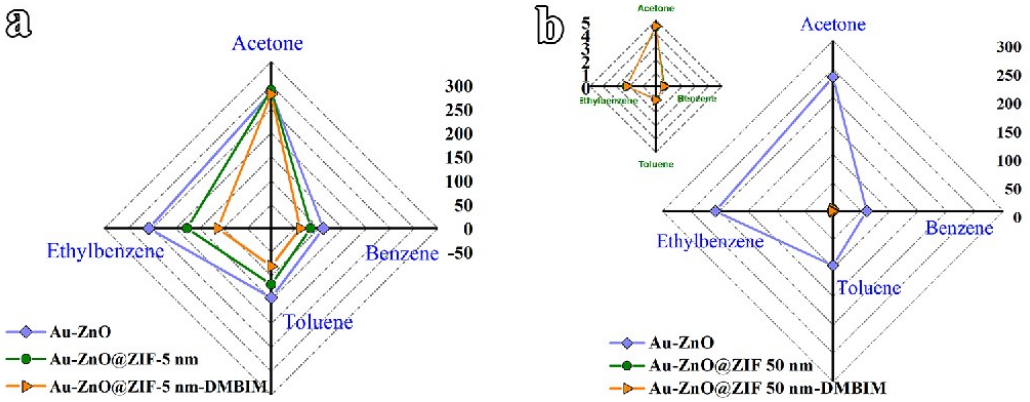

Fig.S18 Responses comparison of different sensors to various gases

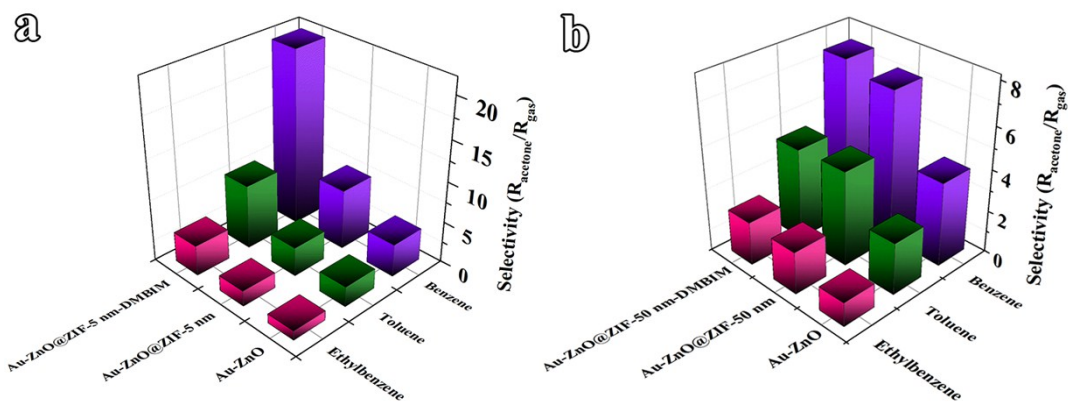

Fig.S19 The selectivity of acetone with four kinds of benzene series: (a) Au-ZnO, Au-ZnO@ZIF 5 nm and Au-ZnO@ZIF 5 nm-DMBIM; (b) Au-ZnO, Au-ZnO@ZIF 50 nm and Au-ZnO@ZIF 50 nm-DMBIM

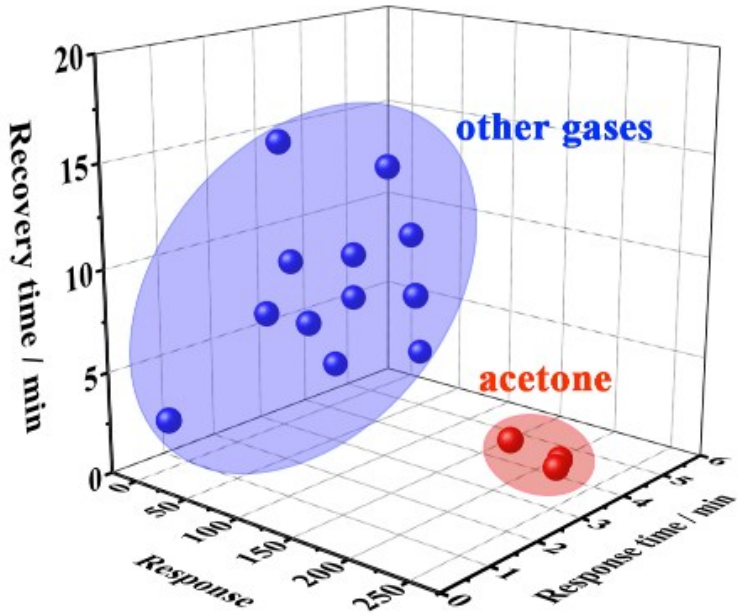

Fig.S20 LDA analysis of the sensor's responses to acetone and benzene series

Table S2 Detailed information of log-log plots of response-concentration for various sensors (LOD: limit of detection (ppm))

	5 nm		30 nm		50 nm	
	ZIF	ZIF-DMBIM	ZIF	ZIF-DMBIM	ZIF	ZIF-DMBIM
β	0.5321	0.7363	0.5517	0.7694	0.4698	0.5538
$\log A_g$	1.1522	0.8158	1.279	0.7908	-0.2945	-0.4398
R^2	0.99	0.98	1.00	1.00	1.00	1.00
LOD	0.0001	0.0034	0.0001	0.0047	0.0315	0.0159

Table S3 Selectivity improvement comparison of acetone toward benzene series of various MOF coated sensors compared with bare Au-ZnO NWA

Core	*Au-ZnO*		*Au-ZnO*		*Au-ZnO*	
Sheath	ZIF 5 nm	+DMBIM	ZIF 30 nm	+DMBIM	ZIF 50 nm	+DMBIM
Benzene	83.8%	440.0%	167.5%	311.0%	78.5%	90.0%
Toluene	43.32%	219.0%	34.7%	115.3%	90.7%	85.59%
Ethylbenzene	30.0%	165.7%	6.5%	78.5%	78.5%	72.0%

Table S4 The sensing responses toward acetone of the devices in this and previous works

Materials	Response (concentration)	Temp./°C	Ref.
Fe-C co-doped WO_3	17 (10 ppm)	300	1
SnO_2/ZnO	21.4 (115 ppm)	300	2
Fe_3O_4-RGO/PIL–PEDOT	1 (saturated vapor)	RT	3
MWCNTs/SnO_2	≈3800 (300 ppm)	250	4
biomorphic SnO_2	7 (10 ppm)	350	5
WO_3 + $HZSM_5$ admix	2.48 (6 ppm)	350	6
NWN ZnO	~ 80 (100 ppm)	300	7
3D spherical porous ZnO	77.5 (100 ppm)	420	8
3-D TiO_2 Nanoflowers	66.58% (700 ppm)	60	9
C/WO_3hollow spheres	10.2 (10 ppm)	300	10
Y-doped ZnO rods	32.2 (100 ppm)	400	11
RuO_2/WO_3NFs	77.61 (5 ppm)	350	12
NiO-decorated TeO_2 nanorod	601% (500 ppm)	125	13
Pt-ZnO NFs	13.07 (5 ppm)	450	14
Single-crystalline α-Fe_2O_3nanospheres	16 (100 ppm)	170	15
GO/ZnO-NR/GO	4.5 (100 ppm)	450	16
mesoporous γ-Fe_2O_3nanoparticles	217 (1000 ppm)	240	17
Pd/AlGaN/GaN	95% (1000 ppm)	150	18
C-Cu_2O crystals	1.7 (5 ppm)	200	19
Pt/Ag-codoped Te_2O_5	5.1 (100 ppm)	150	20
MOF derived ZnO cages	14 (1 ppm)	300	21
NiO-TiO_2	7 (100 ppm)	400	22
ZnO@Au@ZIF-8-DMBIM	231 (100 ppm)	275	This work

References of Table S4

[1] J.-Y. Shen, M.-D. Wang, Y.-F. Wang, J.-Y. Hu, Y. Zhu, Y. X. Zhang, Z.-J. Li and H.-C. Yao, *Sensors Actuators B: Chem*., 2018, 256, 27-37.
[2] T. Rakshit, S. Santra, I. Manna and S. K. Ray, RSC Adv., 2014, 4, 36749-36756.
[3] T. T. Tung, M. Castro, I. Pillin, T. Y. Kim, K. S. Suh and J.-F. Feller, *Carbon*, 2014, 74, 104-112.

[4] S. Ahmadnia-Feyzabad, A. A. Khodadadi, M. Vesali-Naseh and Y. Mortazavi, *Sensors Actuators B: Chem.,* 2012, 166, 150-155.
[5] C. Zhang, J. Wang, R. Hu, Q. Qiao and X. Li, *Sensors Actuators B: Chem*., 2016, 222, 1134-1143.
[6] P. T. Hernández, A. Naik, E. Newton, S. M. Hailes and I. Parkin, *J. Mater. Chem. A*, 2014, 2, 8952-8960.
[7] S. Yi, S. Tian, D. Zeng, K. Xu, X. Peng, H. Wang, S. Zhang and C. Xie, *Sensors Actuators B: Chem.*, 2014, 204, 351-359.
[8] Z. Lin, F. Guo, C. Wang, X. Wang, K. Wang and Y. Qu, *RSC Adv.*, 2014, **4**, 5122-5129.
[9] B. Bhowmik, V. Manjuladevi, R. Gupta and P. Bhattacharyya, *IEEE Sens. J.*, 2016, **16**, 3488-3495.
[10] J.-Y. Shen, L. Zhang, J. Ren, J.-C. Wang, H.-C. Yao and Z.-J. Li, *Sensors Actuators B: Chem*., 2017, 239, 597-607.
[11] P. Yu, J. Wang, H.-y. Du, P.-j. Yao, Y. Hao and X.-g. Li, *J. Nanomater*., 2013, 2013, 4.
[12] K.-H. Kim, S.-J. Kim, H.-J. Cho, N.-H. Kim, J.-S. Jang, S.-J. Choi and I.-D. Kim, *Sensors Actuators B: Chem*., 2017, 241, 1276-1282.
[13] S. Park, G.-J. Sun, H. Kheel, S. Choi and C. Lee, *J. Nanosci. Nanotechno.*, 2016, **16**, 8589-8593.
[14] H.-J. Cho, S.-J. Kim, S.-J. Choi, J.-S. Jang and I.-D. Kim, *Sensors Actuators B: Chem*., 2017, 243, 166-175.
[15] P. Wang, X. Zhang, S. Gao, X. Cheng, L. Sui, Y. Xu, X. Zhao, H. Zhao and L. Huo, *Sens. Actuators B, Chem.*, 2017, **241**, 967-977
[16] B. A. Vessalli, C. A. Zito, T. M. Perfecto, D. P. Volanti and T. Mazon, *J. Alloys Compd.*, 2017, **696**, 996-1003.
[17] J. He, X. Rao, C. Yang, J. Wang, X. Su and C. Niu, *Sens. Actuators B, Chem.*, 2014, **201**, 213-221.
[18] S. Das, S. Ghosh, R. Kumar, A. Bag and D. Biswas, *IEEE Trans. Electron Devices*, 2017, **64**, 4650-4656.
[19] Z. Xie, N. Han, W. Li, Y. Deng, S. Gong, Y. Wang, X. Wu, Y. Li and Y. Chen, *Phys. Status Solidi A*, 2017, **214**, 1600904.
[20] S. Park, G.-J. Sun, H. Kheel, C. Lee and K. Kim, *J. Korean Phys. Soc.*, 2015, **67**, 648-653.
[21] W. Li, X. Wu, N. Han, J. Chen, X. Qian, Y. Deng, W. Tang and Y. Chen, *Sens. Actuators B, Chem.*, 2016, **225**, 158-166.
[22] G.-J. Sun, H. Kheel, S. Choi, S. K. Hyun and C. Lee, *8*., 2017, 17, 4099-4102.

Table S5. Linear discriminant analysis (LDA) of selected sensors

Sample	Au-ZnO	Au-ZnO@ZIF	Au-ZnO@ZIF-DMBIM
Accuracy	92.4%	96.1%	97.2%
Standard deviation	0.0503	0.0632 [a]	0.0330

[a] The value of standard deviation at around 0.05 or lower means high accuracy and good stability of the analysis.